Materials Physics and Mechanics 45 (2020) 1-7 Received: March 11, 2020

ELEMENT-FREE NUMERICAL MODELING WITH DISCRETE GRADIENT AND ITS APPLICATION TO CRYSTAL DEFECTS

Alexander A. Zisman*

Institute of Applied Mathematics and Mechanics, Peter the Great St. Petersburg Polytechnic University,

Polytekhnicheskaya 29, 195251, St. Petersburg, Russian Federation

*e-mail: crism_ru@yahoo.co.uk

Abstract. The gradient operation has been extended to discrete data in terms of nodal coordinates. On this ground, the nodal strains and related stresses are expressed directly in terms of nodal displacements and the stress divergence in terms of nodal stresses. To make use of truly discrete modeling in computational solid mechanics, the stress balance equation is formulated. For a case study, the latter is applied to an edge dislocation where atom positions of a dislocated crystal are taken for nodal points. Both the resulting stress level at the dislocation core close to the theoretical strength and the corresponding core dimensions prove to be realistic physically, whereas the long-range nodal stresses asymptotically approach the virtual continuous fields known in an analytical form.

Keywords: discrete gradient, edge dislocation, element-free model, **s**hape function, stress balance

1. Introduction

Aimed to find approximate continuous solutions of constitutive equations, conventional numerical models treat nodal variables with appropriate continuous approximations. Thus, kinematics in the widely used finite element method (FEM) is formulated with artificial shape functions expressing a displacement field inside each finite element (FE) in terms of its nodal displacements [1,2]. A kind of shape functions is also employed in the element-free extensions of FEM [3-6] aimed to avoid cumbersome re-meshing peculiar to certain applications. The latter few references provide an insight into this rapidly progressing approach though they do not cover a rich variety of related models, where considered nodal points do no longer belong to a certain FE. We will not focus on such works since the present paper should formulate an alternative method, free of a priori continuous approximations. To illustrate performance of this expedient applicable to any type of constitutive equations, its use in solid mechanics will be addressed in the present paper.

An essential prerequisite for the truly discrete modeling is the increasing computational power that makes it possible to treat higher densities of the nodal points and thus allows one to display computation results in terms of the nodal variables only. For the same reason it would be natural to get rid of presumed continuous functions whose non-uniqueness and artificial singularities are essential drawbacks, which limit efficiency of numerical methods. For instance, the mesh-based shape functions are hard to ascribe to actual structural elements of a material which are usually polyhedrons with more than 20 apices. That is why, FEM models of polycrystals subdivide each grain into a lot of conventional primitive elements [7,8] and hence become overcomplicated. As to the meshless shape functions, their definitions are too consumptive [6] for routine engineering problems. It should be remarked, however, that

http://dx.doi.org/10.18720/MPM.4512020_1

the shape functions not only offer continuous solutions, but are also employed to calculate *nodal* variables [1-6] such as stiffness coefficients and related nodal forces. Therefore, a challenging problem arises of how to allow for the material deformation between nodal points using no continuous approximation.

The basic idea of the present paper is to extend the gradient operation, normally involving only infinitesimal surroundings of each considered point, so that it could apply to whole clusters of nodes. Such a way to process discrete data should derive from any local sampling a *uniform* gradient value, thus extracting only a linear part of an underlying continuous field and neglecting unknown residual errors. It is hard to tell in the general case whether such errors, inherent to discrete models, will be less than inaccuracy of presumed shape functions. In any case, denser situated nodal points should increase accuracy of results. The discrete gradient uniquely expressed in terms of nodal coordinates was defined [9] to ensure the least mean square deviation of respective linear field from given nodal values in the differentiation domain. Thus, the nodal strains and, consequently, the stresses can be expressed immediately in terms of nodal displacements and, to get a discrete form of stress balance equation, the stress gradient and then divergence can be found. Previously, the discrete gradient operator was successfully applied to the strain mapping [10] and to imaging crystal curvature [11].

For a case study, the paper considers a stress field of a straight edge dislocation in a solid of finite cross section. First, such a specific application is appropriate to test performance of the discrete modeling for highly singular continuous fields. Besides, it would not be practicable to apply the proposed new method to usual boundary value problems readily tractable with traditional numerical methods. Meanwhile the latter are hardly adapted to simulation of internal microscopic defects (dislocations, inclusions, etc), which are inherent in real structured materials.

The paper is organized as follows. First, the discrete gradient is introduced and its application to nodal variables (displacements, strains, and stresses) is considered. Then, the grounds of the discrete modeling are formulated, and a trial model of the dislocated crystal is described. Next, the calculation results are reported and compared to the long-range stress field of the dislocation, known in an analytic form, and to the relevant physical data on the dislocation core. Finally, potentiality of the proposed method in application to crystal defects and continuous matters, untapped in the case study, is discussed.

2. Use of discrete gradient

Differentiation of discrete data. As shown in [10,12], the discrete gradient can be expressed in terms of partial gradient-vectors

$$\boldsymbol{g}_i = \boldsymbol{r}_i \cdot \Big(\sum_{j=1}^{N} \boldsymbol{r}_j \otimes \boldsymbol{r}_j\Big)^{-1}, \tag{1}$$

where vectors $\boldsymbol{r}_i$ and $\boldsymbol{r}_j$ indicate nodal positions ($i, j=1,2,\ldots,N$), dot and $\otimes$ denote the scalar and tensor products, respectively, and the coordinate origin is selected so that

$$\sum_{j=1}^{N} \boldsymbol{r}_j = 0. \tag{2}$$

In application of Eq. (1) to the nodal displacement vectors $\boldsymbol{u}_i$, the deformation gradient (distortion)

$$\nabla \boldsymbol{u} = \sum_{i=1}^{N} \boldsymbol{g}_i \otimes \boldsymbol{u}_i \tag{3}$$

is expressed. Therefore, the tensors of elastic strain and the rotation at small displacements take on the forms

$$\text{(a) } \varepsilon = \sum_{i=1}^{N} (\boldsymbol{g}_i \otimes \boldsymbol{u}_i + \boldsymbol{u}_i \otimes \boldsymbol{g}_i)/2 \quad \text{(b) } \Omega = \sum_{i=1}^{N} (\boldsymbol{g}_i \otimes \boldsymbol{u}_i - \boldsymbol{u}_i \otimes \boldsymbol{g}_i)/2 \tag{4}$$

the rotation vector dual to Ω being

$$\omega = \sum_{i=1}^{N} (\boldsymbol{g}_i \times \boldsymbol{u}_i)/2, \tag{5}$$

where $\times$ denotes the vector product. It is notable that in case of the same nodal displacements expected zero results of differentiation by Eq. (3), (4) or (5) are ensured by requirement (2).

The considered formalism can apply to tensor variables as well. For instance, if the nodal stresses $\boldsymbol{\sigma}_i$ are derived by Hooke law from respective strains, the stress divergence vector is

$$\nabla \cdot \sigma = \sum_{i=1}^{N} \boldsymbol{g}_i \cdot \boldsymbol{\sigma}_i. \tag{6}$$

According to Eq. (2), this expression also vanishes when the treated field is uniform over a local array of nodes.

Nodal forces by discrete stress balance equation. In application to an arbitrary nodal cluster, Eq. (6) relates the stress divergence to its geometric center. However, the latter may deviate from each considered node whereas the present approach is aimed to treat nodal variables only. Moreover, to enhance accuracy of differentiation, allowance for only immediate neighbors of the considered central node is advisable. To satisfy such conditions with Eq. (2) kept in mind, the neighbors should be symmetrically arranged around a considered point; this, in turn, necessitates *translational symmetry* of the whole nodal pattern. For simplicity, we will use a square grid with unique motive *a*.

Following Eq. (6), the usual stress balance equation

$$\nabla \cdot \sigma + p = 0, \tag{7}$$

where p is a body force, is extended to the nodal stresses by

$$\sum_{i=1}^{N} \boldsymbol{g}_i \cdot \boldsymbol{\sigma}_i + p = 0. \tag{8}$$

However, a discrete force F related to the central node should integrate body forces over an underlying finite volume V and, hence, Eq. (8) takes on the form

$$\sum_{i=1}^{N} \boldsymbol{g}_i \cdot \boldsymbol{\sigma}_i + F/V = 0. \tag{9}$$

Accordingly, in the case of the square pattern with area a^2 over a single node this equation results in

$$f = -a^2 \sum_{i=1}^{4} \boldsymbol{g}_i \cdot \boldsymbol{\sigma}_i, \tag{10}$$

where f is a nodal force per unit thickness.

Procedure of truly discrete modeling. As described in more detail elsewhere [12] and will be illustrated below, the modeling of internal defects by means of the discrete gradient starts from selection of a virtual initial configuration that complies with the presumed geometrical parameters (e.g. Burgers vector of a dislocation) but generally violates the stress balance so that $f \neq 0$ in Eq. (10). Then, proportional to such forces at nodal points, corrective nodal displacements are applied to diminish the stress disbalance, and the resulting configuration is treated in the same way. Such iterations are repeated until f becomes zero with a stated accuracy at each internal node; thereafter the nodal strains and hence stresses are calculated in terms of final nodal displacements.

To evaluate the nodal displacements, related strains and stresses in the initial or any intermediate configuration $\{\boldsymbol{r}_i^*\}$, the latter is compared to the perfect stress-free one $\{\boldsymbol{r}_i^0\}$ and $\boldsymbol{u}_i=\boldsymbol{r}_i^*-\boldsymbol{r}_i^0$ are substituted in Eq. (4a) when considering each node with its next neighbors. According to the trial application considered in what follows, we will use Hooke law for the plane strain case:

$$\begin{aligned}
\sigma_{xx}/G &= \frac{2(1-\nu)}{1-2\nu}\varepsilon_{xx} + \frac{2\nu}{1-2\nu}\varepsilon_{yy},\\
\sigma_{yy}/G &= \frac{2\nu}{1-2\nu}\varepsilon_{xx} + \frac{2(1-\nu)}{1-2\nu}\varepsilon_{yy},\\
\sigma_{xy}/G &= \sigma_{yx}/G = 2\varepsilon_{xy} = 2\varepsilon_{yx},
\end{aligned} \tag{11}$$

where G is the shear modulus and ν is the Poisson ratio. The nodal stresses, thus calculated for neighbors of any considered node, should be substituted in Eq. (10) to derive the corresponding unbalanced force.

3. Modeling finite dislocated crystal

Initial configuration and its relaxation. Under consideration is a straight edge dislocation in the primitive cubic lattice. The model crystal is infinite along the dislocation line, while its upper and lower widths are *101b* and *100b*, respectively, where *b* is the Burgers vector magnitude, and the crystal height is *102b*. The starting configuration, i.e. the arrangements of atoms treated for nodal points, is schematically shown in Fig. 1a. The local coordinates and the related gradient terms, employed in the present work to differentiate discrete data, involve only the nearest neighbors as illustrated in Fig. 1b. For the sake of simplicity, such schemes for four crystal corners, each consisting of three nodes, are omitted. This figure shows also the local distortions of the perfect lattice, which are considered in calculating unbalanced forces in the starting configuration. The forces are due to the simple shearing of elementary cells and prove to localize in the two planes crossing the dislocation core. The nodal coordinates and the related gradients for the next (first) iteration are then calculated, based on the distorted layouts in Fig. 1b.

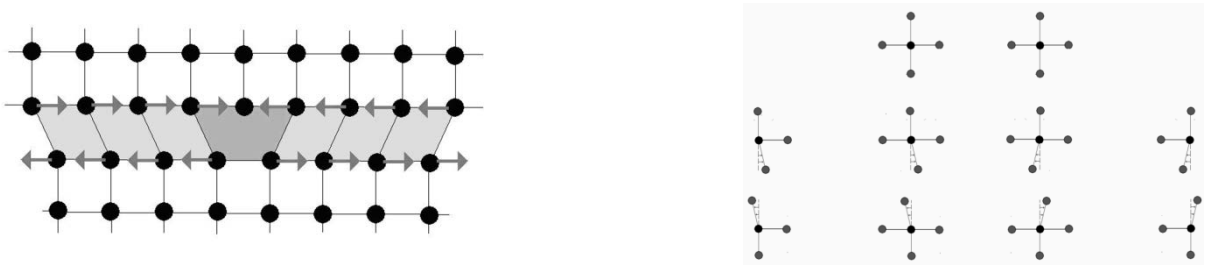

(a) (b)

Fig. 1. Start configuration of the model dislocated crystal with unbalanced nodal forces (a), and the considered layouts of neighbors included in local differentiation domains (b)

The distribution of normalized nodal forces over the model crystal, calculated with $\nu = 1/3$, are mapped in Figs. 2a and 2b for the initial state and after 500 iterations, respectively. As a result of the iteration procedure, unbalanced forces, spread over the crystal, are diminished by three orders. Considering such a relaxation degree satisfactory, one may address the corresponding elastic fields, generated by the dislocation.

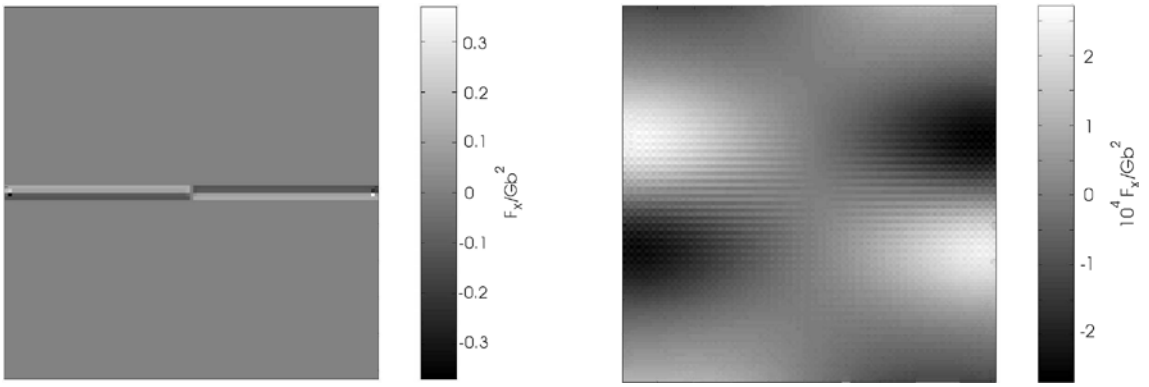

(a) (b)

Fig. 2. Unbalanced forces in the starting configuration of the model dislocated crystal (a) and after 500 iterations of relaxation procedure (b)

Calculated elastic fields. The map of the calculated shear stresses σ_{xy} shown in Fig. 3a fits well the classical (continuum) expression for the long-range stress field of an edge dislocation [13]. Besides, the corresponding elastic displacements allow one to visualize the lateral profile of the finite-model crystal containing the dislocation, as shown in Fig. 3b. Despite minor irregularities at the middle plane due to somewhat insufficient relaxation, this result also proves to be quite realistic.

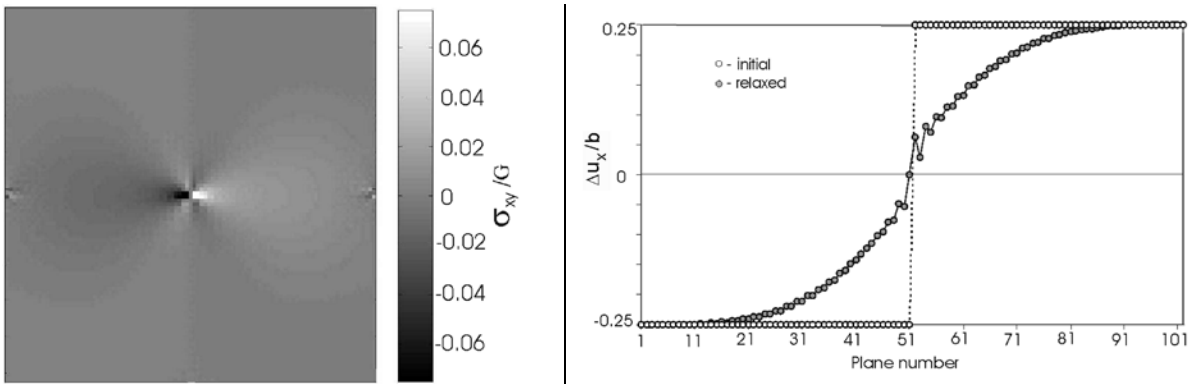

(a) (b)

Fig. 3. Map of the calculated shear stress field over the model dislocated crystal (a) and its lateral profile (b) after 500 iterations of MIF procedure

To analyze the modeling results in the most singular area around the dislocation core, it is expedient to consider the stress distribution in the crystal planes crossing the core. The shear stress σ_{xy} in the horizontal crystal plane touching the core top ($y/b=1$) is plotted in Fig. 4a. The plot provides a very plausible estimate for the core width (*4b*) and corresponds to a realistic theoretical strength of about *0.1G* under the shear stress [13,14]. The tensile stress σ_{xx} in the left half plane under the core (*x/b=-0.5, y/b≤0*) and in the middle vertical half plane over the core (*x/b=0, y/b>0*) is plotted in Fig. 4b. The corresponding core height of *2b* and the theoretical strength of about *0.22G* under the tensile stress also comply satisfactorily to the relevant physical data. It is worth noting that the calculated stresses (Figs. 4a and 4b) are slightly less in magnitude than their continuum counterparts. This is not at all surprising since the considered dislocated crystal is *finite* in plane XY and, hence, its elastic deformation field is more relaxed (less constrained) in comparison to the case of infinite matter.

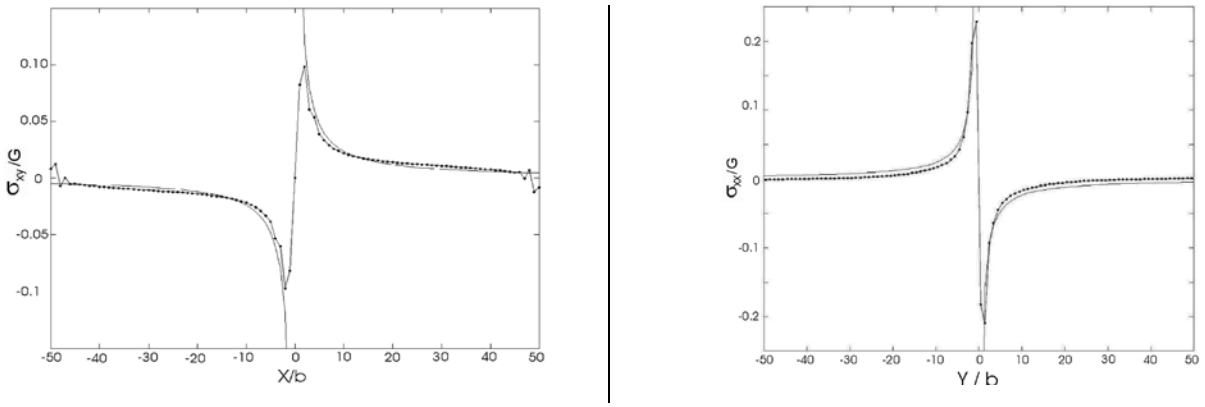

(a) (b)

Fig. 4. Shear stresses σ_{xy} and tensile stresses σ_{xx} in the crystal planes crossing the dislocation core in the horizontal (a) and vertical (b) directions, respectively. The dot and solid lines correspond to the discrete modeling (500 iterations) on the finite crystal and to the analytical solutions for infinite continuum, respectively

4. Discussion

The reported trial application demonstrates efficiency and flexibility of the discrete gradient in numerical modeling. However, a question may arise of why the employed linear elasticity properly works on the essentially microscopic scale of the dislocation core. The point is that the selected starting configuration (Fig. 1a) is satisfactorily close to an actual equilibrium state of the dislocated crystal. Consequently, when treating elementary cells as appropriate continuum fragments, a linear response to their geometrically small deformations remains a good approximation. As to rather strong lattice deformations of the starting configuration in the middle layer of the crystal, as shown in Figure 1a, the corresponding non-linearity does matter only during some number of first iterations and gradually vanishes as the model approaches the balance.

From the physical point of view, the minimum number of nodal points (nearest neighbors), allowed for in differentiation domains by the present model, suggests the minimum cutoff radius of the interatomic interaction. At the same time, one could vary the domain dimensions and, accordingly, the number of involved atoms to analyze effects of crystal type and of atomic bonding on the structure of dislocation core.

The assumption of elastic isotropy employed here, in no way limits applications of the proposed method insofar as the Hook law in its general (anisotropic) form may be used with the same geometrical formalism. Moreover, the same approach seems to be particularly convenient to treat stress singularities in heterogeneous structures (corners and apices of faceted hard particles in deformed materials, dislocations and disclinations on linear junctions of elastically different structural elements, etc).

5. Conclusions

The discrete gradient expressed in terms of the nodal coordinates provides an efficient and flexible tool to differentiate discrete data immediately and hence enables the element-free numerical modeling free of computationally consumptive shape functions. When applied to the nodal displacements, strains and stresses, this approach enables expression of discrete stress balance equation applicable to crystal defects. On this ground, a case study of an edge dislocation in the primitive cubic lattice has been implemented, and the obtained results satisfactorily correspond to both relevant microscopic data on the dislocation core and the known analytical expressions for the long-range stress fields of this defect.

Acknowledgments. *This work was supported by the grant from the Russian Science Foundation (Project No. 19-19-00281).*

References

[1] Zienkievicz OC. The finite element method: from intuition to generality. *Applied Mechanics Reviews*. 1970;23: 249-256.
[2] Gallager RH. *Finite Element Analysis*. New Jersey: Prentice-Hall; 1975.
[3] Belytschko T, Lu Y, Gu L. Element-free Galerkin methods. *International Journal for Numerical Methods in Engineering*. 1994;37(2): 229-256.
[4] Fries TP, Matthjeis HG. *Classification and overview of meshless methods*. Braunsweig: Technical University Braunsweig; 2004.
[5] Chen Y, Lee J, Eskandarian A. *Meshless Methods in Solid Mechanics*. New York: Springer; 2006.
[6] Pan X, Sze KI, Zhang X. An assessment of the meshless weighted least-square method. *Acta Mechanica Solida Sinica*. 2004;17(3): 270-282.
[7] Kanjarla AK, Van Houtte P, Delannay L. Assessment of plastic heterogeneity in grain interaction models using crystal plasticity finite element method. *International Journal of Plasticity*. 2010;26(8): 1220-1233.
[8] Roters F, Eisenlohr P, Hantcherly L, Tjahjanto DD, Bieler TR, Raabe D. Overview of constitutive laws, kinematics, homogenization and multi-scale methods in crystal plasticity finite element modeling: theory, experiments, applications. *Acta Materialia*. 2010;58(4): 1152-1211.
[9] Zisman A, Ermakova N. Deformation and stiffness of finite element with no assumed interpolation. *Journal of the Mechanical Behavior of Materials*. 2006;17: 219-234.
[10] Zisman AA, Ivanov DS, Lomov SV, Verpoest I. Processing discrete data by gradient matrix: application to strain mapping of textile composite. In: Lamon J, Marques AT. (eds.) *Proceedings of 12th European Conference on Composite Materials*. Biarritz; 2006. p.1-8.
[11] Zisman AA, Van Boxel S, Seefeldt M, Van Houtte P. Gradient matrix method to image crystal curvature by processing of EBSD data and trial recognition of low-angle boundaries in IF steel. *Materials Science and Engineering*. 2008;A474: 165-172.
[12] Zisman A. Interpolation-free discrete modeling with gradient matrix: Case study of edge dislocation in linearly elastic crystal. *International Journal of Engineering Science*. 2014;78: 124-133.
[13] Read WT. *Dislocations in Crystals*. New York: McGraw-Hill; 1953.
[14] Dieter GE. *Mechanical Metallurgy*. New York: McGraw-Hill; 1986.